

ASSESSMENT OF POWER SYSTEM GLOBAL STABILITY DETERMINED BY UNSTABLE LIMIT CYCLE

Masayuki Watanabe, Yasunori Mitani, Kiichiro Tsuji
Graduate School of Engineering, Osaka University
Osaka, Japan
masa-w@polux.pwr.eng.osaka-u.ac.jp

Abstract - This paper presents a method to investigate the power system global stability formed by an unstable limit cycle, which can be calculated by means of Hopf bifurcation theory. The stability region is evaluated on the δ - ω phase plane including the effect of field winding flux linkage change. The global stability is assessed in comparison with the classical transient stability in some multi-machine power systems with longitudinally interconnected configuration. A control strategy to keep the system trajectory inside of globally stable region after a large disturbance by controlling the field voltage is developed from the results.

Keywords - power system stability, nonlinear system, Hopf bifurcation, excitation control

1 INTRODUCTION

POWER system is a dynamic system, which includes several kinds of nonlinear elements. Transient stability is a typical example originated in the nonlinearity of power swing. On the other hand, the use of nonlinear analysis method based on the Hopf bifurcation theory [1], [2] tells us the existence of a limit cycle around an operating point and the stability of limit cycle. It has been investigated in the literatures so far that the structure of limit cycles results from the specific AVR operations [3], the nonlinearity of damping coefficient [4], the effect of induction machine load [5] and so on [6].

In this paper power system global stability formed by an unstable limit cycle, is evaluated. The limit cycle can be detected based on the Hopf bifurcation theory. Here, a method to evaluate the global stability on the δ - ω phase plane similar to the ordinary transient stability analysis, is developed. Thus, the global stability is investigated in comparison with the classical transient stability assessment. The limit cycle discussed here results from the excitation control. Therefore, it is important to consider the effect of flux linkage change in the field winding in addition to the δ - ω variables. In the classical method, the flux linkage of field winding has been treated to be constant after a disturbance. On the other hand, by observing the behavior of power system with an unstable limit cycle, it is found that the system trajectory forms a kind of orbit at a level in the direction of field winding flux linkage. And the level is gradually elevated with the power oscillation. Thus, it is considered that the system condition varies with the quasi-static flux linkage of field winding, which affects the structure of nonlinear limit cycle.

In this paper the global stability is investigated by as-

suming that the flux linkage of field winding around the limit cycle is quasi-static, that is, the response of field winding flux linkage is much slower than that of generator swing. Thus, the limit cycle is evaluated by changing the initial field voltage as a parameter. Then, it becomes possible to evaluate the global stability boundary formed by the unstable limit cycle as a function of variables of δ , ω and quasi-static e'_q . This method has been applied to one-machine and infinite bus system in our previous work [9], which demonstrated an accurate evaluation of global stability boundary associated with the unstable limit cycle. In this paper, the method is extended and applied to some multi-machine power systems with longitudinal interconnections, in which an electro-mechanical mode with low frequency is dominant. In such a case the dynamics of dominant mode is almost equivalent to the dynamics of one-machine and infinite bus system. Finally, a method to stabilize the power system with a stability problem associated with the unstable limit cycle has been developed by setting the reference value of field voltage appropriately according to the results of stability region analysis.

2 HOPF BIFURCATION AND POWER SYSTEM STABILITY

Consider a nonlinear dynamical system described by following equation

$$\dot{x} = f(x, p), x \in \mathbf{R}^n \quad (1)$$

where p is a parameter. A value of the parameter $p = p_0$ at which the vector field f loses its structural stability is called a bifurcation point. If Df (the linearization of f at (x_0, p_0)) has a simple pair of pure imaginary eigenvalues at $p = p_0$, with all other eigenvalues lying off the imaginary axis, this bifurcation is called Hopf bifurcation. When the differential equations that describe the stable modes are approximated by algebra equations, the unstable oscillatory mode is expressed approximately as a second order nonlinear equation. Then, this system can be cast by a smooth change of coordinates into the polar form called Normal Form [1], [2].

$$\dot{r} = (d\mu + ar^2)r \quad (2)$$

$$\dot{\theta} = \omega + c\mu + br^2 \quad (3)$$

If $d \neq 0$, there is a bifurcation at $\mu = 0$. Since the first equation does not depend on θ , we see immediately that there are periodic orbits, $r = \sqrt{-d\mu/a}$. The bifurcation is said to be subcritical if the periodic solution is unstable

and supercritical if it is stable. Figure 1 shows an example of bifurcation diagram.

In a power system, the Hopf bifurcation and limit cycles appear when a certain excitation system is considered. The Hopf bifurcation theory is applicable to the system with the instability of dominant mode. The mode becomes unstable as the power flow of the system increases, which corresponds to the increase of μ in Figure 1. In this paper, the global stability formed by the unstable limit cycle in longitudinally interconnected power systems is investigated on δ - ω phase plane.

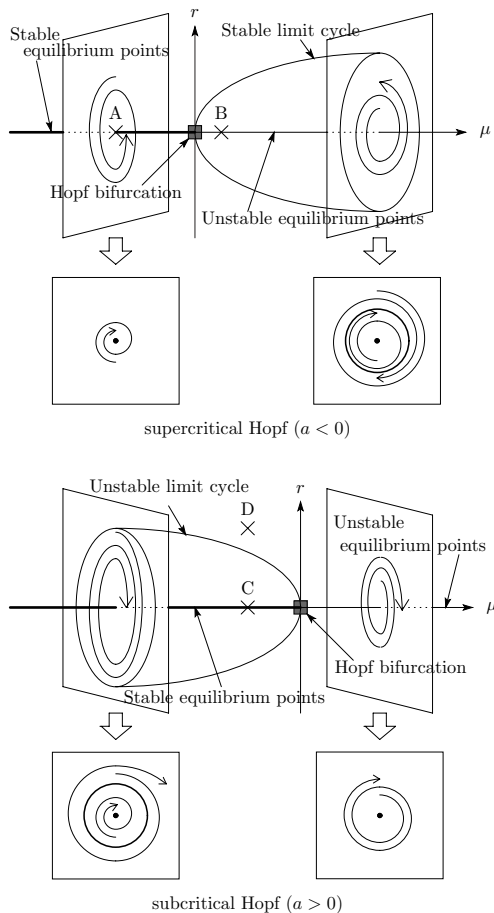


Figure 1: Bifurcation diagrams.

When power system has a supercritical Hopf bifurcation, a stable limit cycle exists around the unstable equilibrium point as shown in Figure 1. Usually, the system is operated at a stable equilibrium point, for example, at point A in Figure 1. However, even if operated at point B, the system does not lose the synchronization and is kept to operate with a sustained oscillation, since the system trajectory is trapped by the stable limit cycle.

On the other hand, when the system has a subcritical Hopf bifurcation, an unstable limit cycle exists around the stable equilibrium point. And this limit cycle forms a global stability boundary. If the system state moves to point D, that is, the outside of the limit cycle by a large disturbance when the system is operated at stable equilibrium point C, the system trajectory is distracted from the limit cycle and finally the generator loses the synchronization.

Thus, the inner area of unstable limit cycle corresponds to stable region. The stable region occasionally can be much narrower than the region calculated by the classical transient stability analysis method.

Accordingly, it is important in stability analysis to grasp the property of limit cycle around the operating point when the system condition is near the Hopf bifurcation point. In particular the unstable limit cycle affects the global stability. In the subsequent discussions emphasis is placed on the numerical analysis of unstable limit cycle in power systems.

3 GLOBAL STABILITY ANALYSIS CONSIDERING THE RESPONSE OF FIELD WINDING FLUX LINKAGE

Dynamic characteristics of a generator are expressed by oscillatory property of a rotor represented by state variables δ and ω , property of armature winding, property of damper winding, and property of field winding. The power system stability described here is mainly decided by oscillatory characteristic of the rotor. Compared to this characteristic, transient responses of armature and damper windings damp out in a very short time after a disturbance. On the other hand, the response of field winding is slow but varies with δ and ω . As a result, the system stability should be evaluated on δ - ω phase plane with taking account of the variation of flux linkage in field winding.

Figure 2 shows an example of the behavior of power oscillation observed in a three-machine longitudinal interconnected power system that is to appear in later discussions. The system has a subcritical Hopf bifurcation and hereby an unstable limit cycle, which is depicted at the same time.

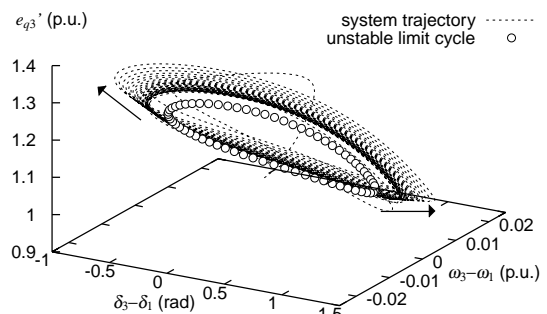


Figure 2: System response and unstable limit cycle.

The limit cycle calculated for the system based on the initial condition is formed at a level of direction slightly leaning from the e'_q axis. Once a disturbance occurs, after an initial transient, the system trajectory seems to be attracted by the limit cycle and forms the same kind of orbit level. However, the e'_q level of system trajectory is a little higher than the e'_q level of unstable limit cycle. The level of system trajectory is gradually elevated and enlarged with the electro-mechanical oscillation (see Figure 2). Thus, the comparison of the system trajectory with the unstable limit cycle is useless for the evaluation of stability region. Therefore, the authors proposed a method

to calculate the stability boundary formed by the unstable limit cycles for different field voltage levels [9], which has been applied to a one-machine and infinite bus system. Some numerical studies demonstrate the accuracy of method by comparing the system trajectory after the initial transient with the calculated boundary.

In this paper, the method is modified so as to apply it to multi-machine power systems with longitudinal interconnections.

4 ASSESSMENT IN A THREE-MACHINE SYSTEM

4.1 Power System Model

As mentioned in chapter 2, the Hopf bifurcation theory is applicable to the system with the instability of dominant mode. So, it is difficult to analyze the system which the multiple modes become unstable simultaneously. However, when the specific mode becomes unstable as the power flow of the system increases even in multi-machine system, the oscillatory mode is equivalently explained as the oscillation in a one-machine and infinite bus system. Thus, a similar method is applicable.

Figure 3 shows the configuration of a three-machine longitudinally interconnected power system used in this study. In the longitudinal system, the low frequency oscillation between both end generators tends to become unstable. Therefore, the analysis method based on Hopf bifurcation theory is applicable. This method can be applied to other power systems which show the instability associated with the slow damping oscillatory mode, not restricted to longitudinal structure like this example.

Here, the model used for numerical studies is explained. The generator model is represented by the fifth order Park's equations with a set of swing equation, the response of field winding and two damper windings in d - q axes.

$$\begin{aligned}
T'_{do} \frac{de'_q}{dt} &= -\frac{x_d - x'_d}{x'_d - x''_d} e'_q + \frac{x_d - x'_d}{x'_d - x''_d} e''_q + E_{fd} \\
T''_{do} \frac{de''_q}{dt} &= -e''_q + e'_q - (x'_d - x''_d) i_d \\
T''_{qo} \frac{de''_d}{dt} &= -e''_d + (x_q - x''_q) i_q \\
M \frac{d\omega}{dt} &= -D(\omega - 1) + P_m \\
&\quad - \{e''_q i_q + e''_d i_d + (x''_q - x''_d) i_d i_q\} \\
\frac{d\delta}{dt} &= \omega_0(\omega - 1)
\end{aligned} \tag{4}$$

An AVR shown in Figure 4 is considered. Table 1 shows system constants.

An assumed system disturbance is a three phase ground fault at a circuit near the generator G_3 in the double circuit transmission line (see \times in Figure 3). The fault circuit is cleared at several cycles after the fault occurred.

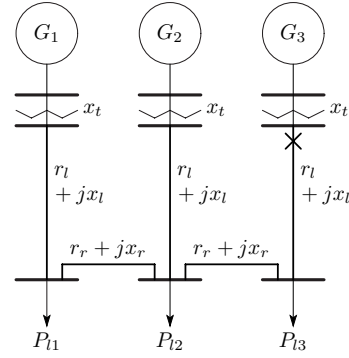


Figure 3: Three-machine interconnected power system.

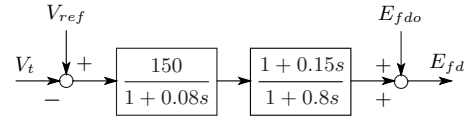


Figure 4: Block diagram of AVR.

Generator: 4000MVA (four 1000MVA generators) base		
$x_d = 1.79$ (p.u.)	$x'_d = 0.355$ (p.u.)	$x''_d = 0.275$ (p.u.)
$x_q = 1.66$ (p.u.)	$x'_q = 0.570$ (p.u.)	$x''_q = 0.275$ (p.u.)
$T'_{do} = 7.90$ (s)	$T''_{do} = 0.032$ (s)	$T''_{qo} = 0.055$ (s)
$D = 0.0$ (s)	$M = 7.53$ (s)	
Transmission System: 4000MVA, 500kV base		
$x_t = 0.14$ (p.u.)	$x_l = x_r = 0.126$ (p.u.)	
$r_l = r_r = 0.00421$ (p.u.)		

Table 1: System constants.

4.2 Assessment of Global Stability

In a multi-machine system, a swing bus as the reference of phase angle should be selected to eliminate the dynamics of center of inertia. Here, the phase angle of the generator G_1 is selected as the reference since the dominant oscillation is formed by generators between both ends in a longitudinal system. The nonlinear characteristics of the system are evaluated on the phase plane of $\tilde{\delta} = \delta_3 - \delta_1$ and $\tilde{\omega} = \omega_3 - \omega_1$. All of bifurcation diagrams are calculated by using the nonlinear system analysis software package, AUTO [7]. Figure 5 shows the bifurcation diagram of the power system described by changing the mechanical power input P_{m3} of the generator G_3 as a parameter, where the limit cycles are represented by the maximum envelop of orbit.

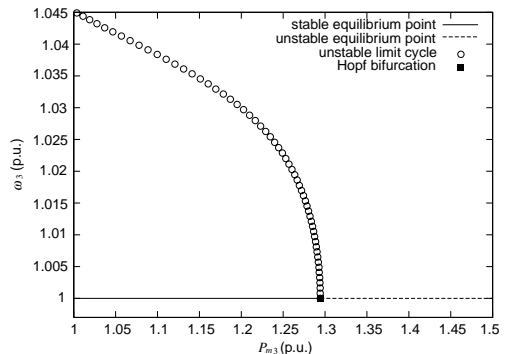


Figure 5: Bifurcation diagram.

Figure 5 shows that this is the subcritical case, that is, an unstable limit cycle exists around the stable equilibrium points. Therefore, the system may lose the synchronization if a large disturbance occurs when it is operating near the Hopf bifurcation point.

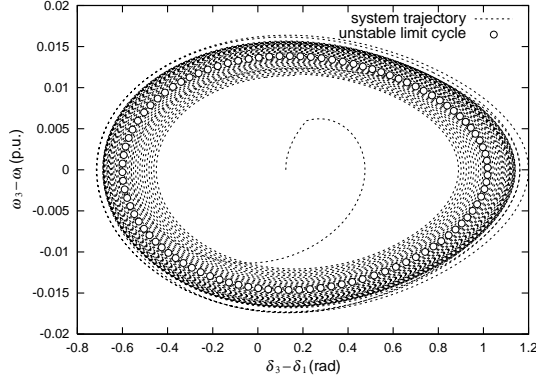


Figure 6: System response and unstable limit cycle.

Figure 6 shows the unstable limit cycle and the system trajectory triggered by a 3LG during 0.082 s, both of which are projected on the δ - ω phase plane. The system is initially operated at $P_{m1} = 0.915$ (p.u.), $P_{m2} = P_{l1} = P_{l2} = 0.9$ (p.u.), $P_{m3} = P_{l3} = 1.28$ (p.u.) corresponding to the slightly stable side of Hopf bifurcation point. The unstable limit cycle projected on the plane is depicted as small white circles. It should be noted that the limit cycle exists inside of conventional separatrix determined by the classical transient stability analysis, which implies that the unstable limit cycle forms a global stability boundary. In Figure 6 the trajectory just after the disturbance initially stays outside of limit cycle. However, the power swing is gradually attenuating after it passed across the unstable limit cycle. This implies that the evaluation of stability region by means of unstable limit cycle projected on the δ - ω phase plane is not completely correct.

As stated above, we treat e'_q as a quasi-static variable since the response of field winding flux linkage is much slower than that of generator swing. The level of field flux linkage that gradually changes during the generator swing, is represented as the change of initial field voltage. Figure 7 shows the variations of unstable limit cycle for different initial filed voltage settings by changing the reference voltage V_{ref} of the AVR in the generator G_3 . Note that almost same result is obtained when V_{ref} of G_1 is changed as a parameter.

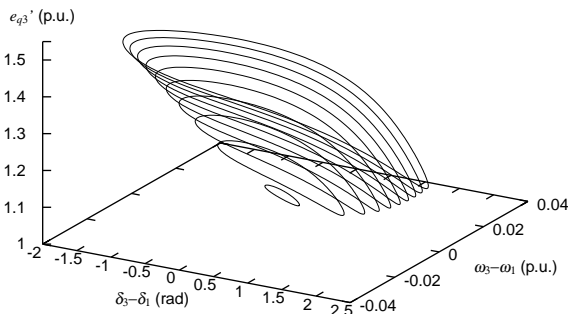


Figure 7: Unstable limit cycles for different initial filed voltage settings.

Different levels of limit cycle are formed as the field winding flux linkage changes. The system stability can be evaluated by comparing the system trajectory with the limit cycle in the same level of field flux linkage. Figure 8 shows the original limit cycle and the limit cycle with considering the change of flux linkage (call this the modified limit cycle), which are projected on δ - ω phase plane. The system trajectory between 4.3 sec and 5.3 sec after the disturbance are depicted on the same plane. The results show that the system state has been outside of the original limit cycle, while the modified limit cycle correctly includes the trajectory inside.

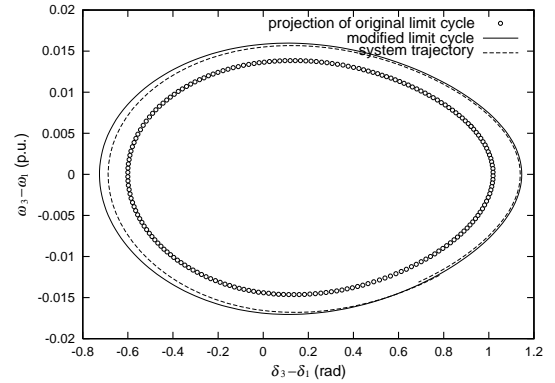


Figure 8: Comparison of stability region between original and modified limit cycles.

4.3 Second example in a three-machine model

The method has been applied to the system in Figure 3, where a limiter for the field voltage of AVR with a PSS shown in Figure 9 is considered.

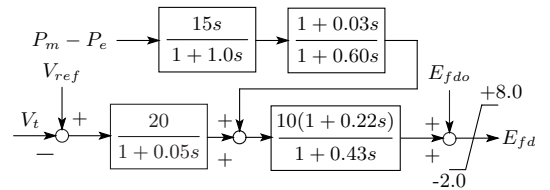


Figure 9: Block diagram of AVR and PSS.

Figure 10 shows the bifurcation diagram by changing the mechanical input P_{m3} of generator G_3 as a parameter. Without the limiter, the system has a supercritical Hopf bifurcation, which implies that the system has a sustained oscillation but does not lose the synchronization when it is operated at an unstable equilibrium point. In case with the limiter of field voltage, the bifurcation characteristic changes from supercritical to subcritical as shown in Figure 10. This has to be important information on the global stability assessment, since the stable region is reduced by the unstable limit cycle.

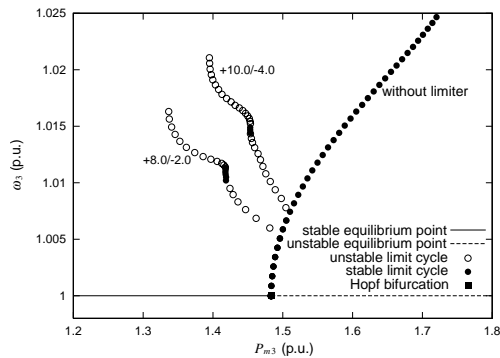


Figure 10: Bifurcation diagram.

Here, consider that the system is operated at $P_{m1} = 0.917$ (p.u.), $P_{m2} = P_{l1} = P_{l2} = 0.9$ (p.u.), $P_{m3} = P_{l3} = 1.43$ (p.u.), which is slightly stable side of Hopf bifurcation point. Figure 11 shows the variations of unstable limit cycle for different initial filed voltage settings by changing V_{ref} of AVR in the generator G_3 as a parameter. For the stability analysis the system trajectory is compared with the limit cycle at the same level of field flux linkage. The result is shown in Figure 12. The system trajectory is drawn between 1.8 sec and 2.6 sec after the disturbance, where the fault was cleared at 0.054 sec. In this case, the system is unstable and finally it is to lose the synchronization after growing oscillations. However, the original limit cycle informs that the system is still stable, while the system stability is evaluated correctly by the modified limit cycle.

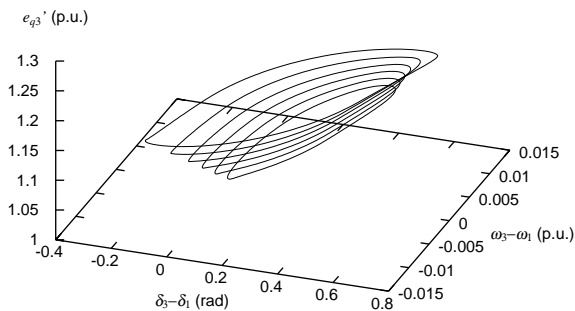


Figure 11: Unstable limit cycles for different initial filed voltage settings.

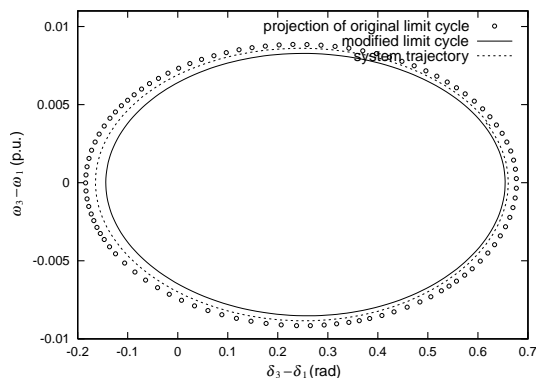


Figure 12: Comparison of stability region between original and modified limit cycles.

The criteria of stability on the phase plane is not easy to obtain since the level of field winding flux linkage can not be easily determined. Therefore, a method to de-

fine the stability region clearly, is derived here from the viewpoint that each limit cycle is analogous. First, take a cross section of dimension 2 at the maximum point of $\tilde{\omega} = \omega_3 - \omega_1$ in Figure 11. The cross section is defined as the $\tilde{\omega}-e'_{q3}$ plane. Then, we obtain a group of intersections, which are drawn by a solid line in Figure 13. The map of system trajectory on the cross section is obtained in a same manner. Two examples of the map are depicted in Figure 13; in stable case the fault was cleared at 0.052 sec and at 0.054 sec in unstable case. Thus, the global stability boundary on $\omega-e'_q$ plane is defined, in which the system is stable if the system trajectory map stays in the left hand side of boundary, and vice versa. The stable case map converges into the stable equilibrium point.

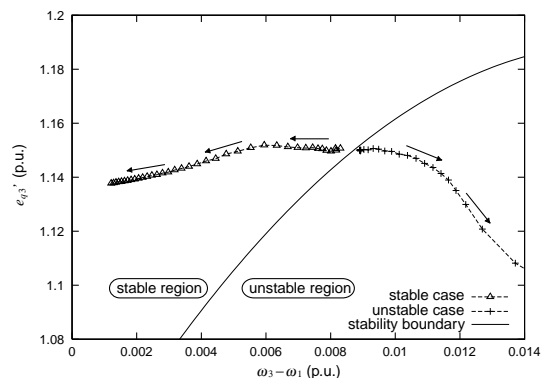


Figure 13: Stability boundary represented on $\omega-e'_q$ plane.

Figure 14 shows the time-domain simulation results in case with the limiter of filed voltage and in case without the limiter. Since there is no unstable limit cycle around the operating point in case without the limiter, the oscillation damps out. In case with the limiter the oscillation is growing and finally the system loses synchronization.

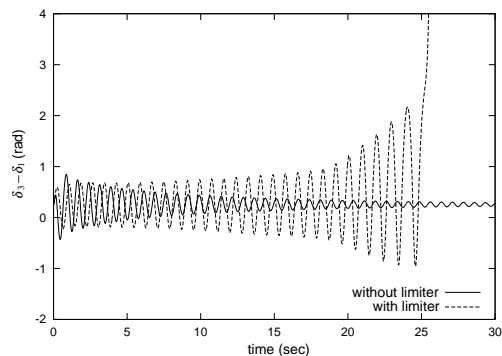


Figure 14: Oscillations of generator phase angle.

5 INVESTIGATION IN A TEN-MACHINE SYSTEM

5.1 System Model

Figure 15 shows the configuration of a ten-machine longitudinally interconnected power system. The generator model is represented by the fifth order Park's model. Each generator is equipped with the AVR shown in Figure 16. Table 2 shows system constants. A three phase

ground fault at the transmission line near the generator G_1 is considered as a disturbance.

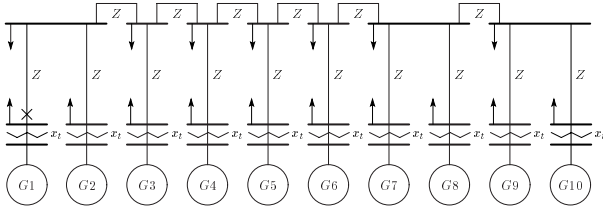


Figure 15: Ten-machine system.

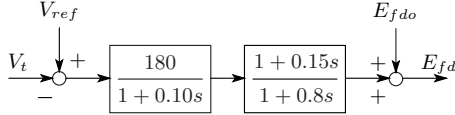


Figure 16: Block diagram of AVR.

Generator: Park's 5th model, 1000MVA base		
$x_d = 1.79$ (p.u.)	$x'_d = 0.35$ (p.u.)	$x''_d = 0.25$ (p.u.)
$x_q = 1.79$ (p.u.)	$x'_q = 0.35$ (p.u.)	$x''_q = 0.25$ (p.u.)
$T'_{do} = 4.86$ (s)	$T''_{do} = 0.042$ (s)	$T''_{qo} = 0.042$ (s)
$D = 0.0$ (s)	$M = 7.00$ (s)	
Transmission System: 1000MVA, 500kV base		
$x_t = 0.14$ (p.u.)		
$Z = 0.0042 + j0.126$ (p.u.)	double circuit	

Table 2: System constants of ten-machine system.

5.2 Numerical Method to Calculate Limit Cycle by Using Generator Swing Data

In case of a relatively small power system like a three-machine system as shown in Figure 3, the unstable limit cycle can be calculated by using a nonlinear system analysis software package, such as AUTO[7]. However, it becomes difficult to apply this method to a large-scale system, since it is difficult to express all the state equation describing the large-scale power system with only explicit functions of state variables. The authors have developed a numerical method to approximate the system equations by polynomial of δ and ω [8]. The approximation is carried out with a set of generator swing data (P_e , δ and ω) by applying the least squares method.

$$\begin{aligned} \dot{x}_1 &= k_1 x_1 + k_2 x_2 + k_3 x_1^2 + k_4 x_2^2 + k_5 x_1 x_2 \\ &\quad + k_6 x_1^3 + k_7 x_2^3 + k_8 x_1^2 x_2 + k_9 x_1 x_2^2 \quad (5) \\ \dot{x}_2 &= x_1 \quad (6) \end{aligned}$$

where, $x_1 = \omega_r(\omega_1 - \omega_{10})$, $x_2 = (\delta_1 - \delta_{1i}) - (\delta_{10} - \delta_{10i})$; subscript i means the initial equilibrium point. Since the oscillation mode associating with the swing between both end-generators tends to become unstable when some power flows are heavy, the phase angle of the generator G_{10} is selected as the reference of phase angle. By acquiring data set of e'_q together with (P_e , δ and ω) data for applying the least squares method above, the relation between e'_q and ω_{\max} can be estimated; e'_q is interpolated by a quadratic function of ω_{\max} . The detail of limit cycle is

evaluated by analyzing the system of (5) and (6). As a result, the radii of limit cycle are calculated by

$$x_1 = \sqrt{k_1 k_2 / a} \sin(\theta + \pi/4) \quad (7)$$

$$x_2 = \sqrt{-k_1 / a} \sin(\theta + 3\pi/4) \quad (8)$$

where,

$$a = \frac{k_5(k_2 k_3 - k_4) - 3k_2^2 k_6 + k_2 k_9}{4k_2} \quad (9)$$

Accordingly, the maximum ω of limit cycle and corresponding e'_q are obtained. By acquiring the system swing data with changing the initial field voltage as a parameter, the limit cycles for different levels of field winding flux linkage, that is, the stability region is finally determined.

This numerical method is applied to a ten-machine system shown in Figure 15. Figure 17 shows the calculation results of stability boundary when the system is operated at $P_m = 0.9$ (p.u.), $V_{ref} = 1.03$ (p.u.). The system trajectories when the system is stable and unstable are also drawn. The fault clearing time is 0.026 sec in the stable case, 0.027 sec in the unstable case. The corresponding oscillations of generator phase angle are shown in Figure 18. The results show that the numerical method by using generator swing data detects the correct stability boundary associated with the unstable limit cycle.

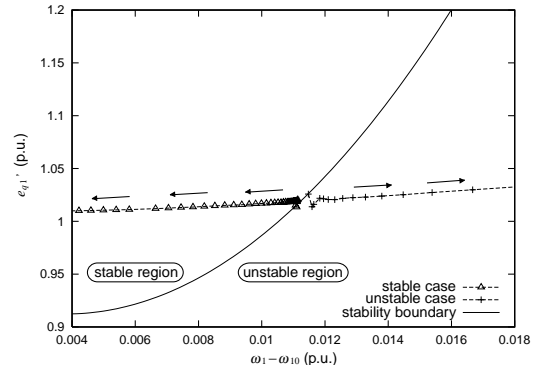


Figure 17: Stability boundary approximately obtained by using generator swing data.

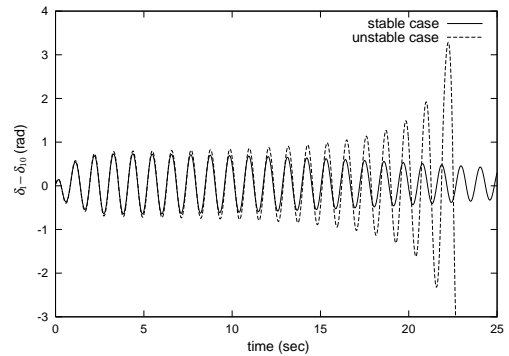


Figure 18: Oscillations of generator phase angle.

5.3 Control of Power System

It is predicted from the stability boundary in Figure 17 that the system can be controlled toward the stable region

by enlarging e'_{q1} , which is realized by enhancing the field voltage. Then, a control to increase the reference voltage in AVR is applied when the system is just outside of the stability boundary. Figure 19 shows an example of control, where the reference voltage in AVR of generator G_1 has been raised from $V_{ref} = 1.03$ (p.u.) to $V_{ref} = 1.05$ (p.u.) at several seconds after the disturbance. In this case the system is unstable without the control. As a result of control the system state is shifted into stable region from unstable region and finally goes toward the post-fault equilibrium point.

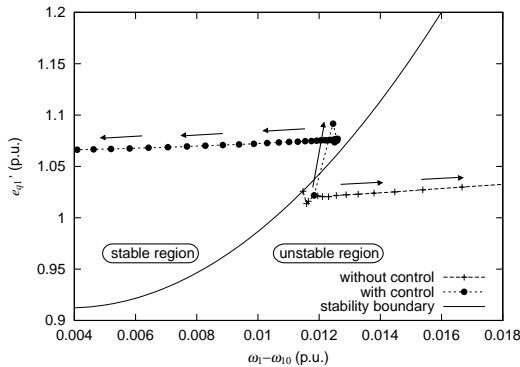


Figure 19: Stabilizing effect by voltage control.

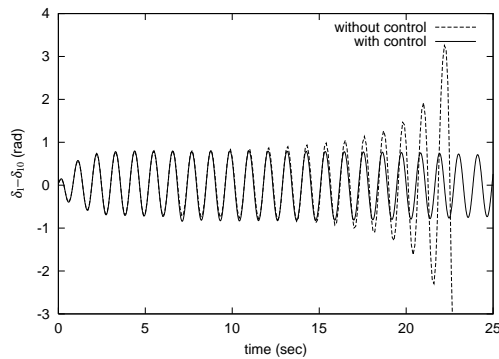


Figure 20: Oscillations of generator phase angle.

6 CONCLUSIONS

A global stability evaluation method based on the nonlinear system analysis is developed. The evaluation is carried out on δ - ω phase plane, by which the results can be compared with the classical transient stability analysis. The error of stability boundary associated with the unstable limit cycle projected on δ - ω plane is modified by considering the variation of field winding flux linkage.

The stability boundary is defined by a map of limit cycle set on the cross section, which is represented on ω - e'_{q1} plane. A control scheme by the adjustment of field voltage to keep the power system in the stable region, is also investigated.

The methods are applied to the nonlinear analysis of stability associated with a low frequency oscillation in longitudinally interconnected systems. Correct evaluation and feasible control results are demonstrated in numerical studies using three-machine and ten-machine systems.

The methods are applicable to other systems, in which an electro-mechanical mode with low-frequency is dominant. The last numerical method is effective for the analysis of more large-scale power systems, which are difficult to analyze the stability region by using the nonlinear analysis software package.

ACKNOWLEDGEMENT

This research was partially supported by Japan Society for the Promotion of Science (JSPS), Grant-in-Aid for Scientific Research (C), 12650277, 2001.

REFERENCES

- [1] J. Guckenheimer, P. Holmes, "Nonlinear oscillations, dynamical systems, and bifurcations of vector fields", Springer-Verlag, New York, Applied Mathematical Sciences 42, 1983.
- [2] S. Wiggins, "Introduction to Applied Nonlinear Dynamical Systems and Chaos", Springer-Verlag, New York, Texts in Applied Mathematics 2, 1990.
- [3] C. D. Vournas, M. A. Pai, P. W. Sauer, "The effect of Automatic Voltage Regulation on the bifurcation evolution in power systems", IEEE Transactions on Power Systems, Vol.11, No.4, November, 1996, pp.1683–1688.
- [4] E. H. Abed, P. P. Varaiya, "Nonlinear Oscillations in power systems", International Journal of Electrical Power & Energy Systems, Vol.6, No.1, January, 1984, pp.37–43.
- [5] V. Ajjarapu, B. Lee, "Bifurcation theory and its application to nonlinear dynamical phenomena in an electrical power system", IEEE Transactions on Power Systems, Vol.7, No.1, February, 1992, pp.424–431.
- [6] J. C. Alexander "Oscillatory solutions of a model system of nonlinear swing equations", International Journal of Electrical Power & Energy Systems, Vol.8, No.3, July, 1986, pp.130–136.
- [7] E. J. Doedel, A. R. Champneys, T. F. Fairgrieve, Y. A. Kuznetsov, B. Sandstede, X. Wang, "AUTO97: Continuation and bifurcation software for ordinary differential equations (with HomCont)", February, 1997.
- [8] Y. Mitani, P. Miao, K. Tsuji, "A Numerical Method to Evaluate Bifurcation Aspects around Generator Stability Limit", Proc. of ISCAS2000 in Geneva, Switzerland.
- [9] M. Watanabe, P. Miao, Y. Mitani, K. Tsuji, "Assessment and Control of Power System Global Stability Determined by Unstable Limit Cycle", 2001 IEEE Porto Power Tech Proceedings.